Simulation of Orientation-Dependent Etching of Silicon Using a New Step Flow Model of 3D Structuring

A. Horn*, H. Schröder**, E. Obermeier**, G. Wachutka*

*Institute for Physics of Electrotechnology, Munich University of Technology, Arcisstrasse 21, D-80290 München, Germany, horn@tep.ei.tum.de
**Technical University of Berlin, MAT, Sekr TIB 3.1, Gustav-Meyer-Allee 25, D-13355 Berlin, Germany

ABSTRACT

We present a new model of three-dimensional orientation-dependent etching of $Si_{\{100\}}$. Recent experimental results suggest to conceive etching as a "peeling" process of terraced planes, leading to the concept of a "step flow model of 3D structuring". In particular, a first implementation in a numerical simulation tool allowed us to correctly reproduce the observed details of convex corner (CC) undercutting in pure aqueous KOH solutions (Fig. 2). The new aspect incorporated in this model is the experimental finding that the so-called "fast etching planes", which commonly are referred to as cause of the characteristic shape of underetched convex corners of the etchmask, are not really crystallographic planes.

Instead these areas, denoted as "B" in Fig. 2, are the envelope surfaces of a bunched sequence of <110> oriented steplines with kink sites on the intersecting {111} planes. The typical morphology occurring at underetched convex corners is correctly retrieved by our simulation approach, as it can be verified by comparison with SEM micrographs (Fig. 1, Fig. 2).

Keywords: Orientation-Dependent Wet Chemical Etching, Silicon, 3D-Simulation.

1 INTRODUCTION

The orientation-dependent etching of silicon in aqueous KOH solutions is still one of the fundamental techniques in silicon bulk micromachining.

However, the characteristic shape and morphology of the etch front at underetched convex corners cannot be satisfactorily explained by the commonly used models of the etching mechanism. Fig. 1 displays a SEM micrograph of an anisotropically etched mesa structure on {100}-silicon. At each convex corner, the etch front is composed of areas with different surface morphology. One type of areas exhibit a smooth and regular fine structure, while others look quite rough and have irregular shape. This finding cannot be described and consistently explained by the well-known and widely accepted differential-geometrical simulation approaches [1,2,3,4]. But, convex corner undercutting seems to be the key to understand the anisotropic etching process as a whole, which in turn is indispensable for the accurate and efficient design of mask layouts for increasingly complex mircomachined structures.

To this end, we present in this paper the numerical implementation of a new "step flow model of 3D structuring", which can accurately reproduce the time evolution of the etch front at length scales relevant for micromechanical structures.

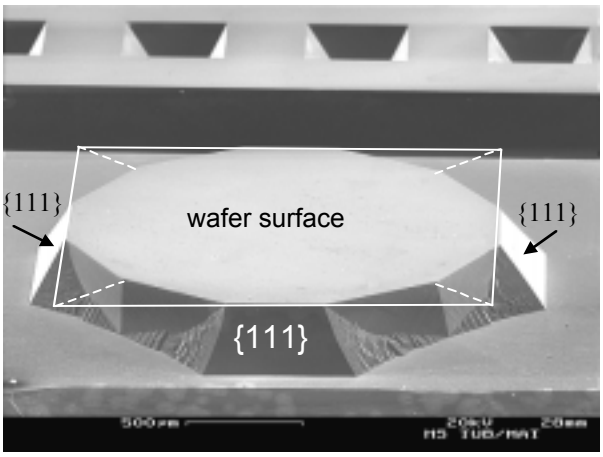

Fig. 1: SEM micrograph of a mesa structure with four underetched convex corners as obtained from a square etch mask. The white lines indicate the location of the mask before it was removed.

2 NUMERICAL MODELLING

2.1 Step Flow Model of 3D Structuring

The anisotropic etching process can be understood as a step flow process [5,6], in which a stepped sequence of terraces formed by stable {111} planes is attacked at the steps and, thereby, successively peeled off in lateral direction [7]. A convex corner of an etch mask acts as a point of instability, where two kink sites are generated. These are the initial points at which the lateral ablation of the underlying {111} planes originates. With progressing removal of the etch bottom in [100]-direction new kink sites emerge and further steps are generated which

contribute to the lateral peel-off process. Fig. 2 shows a zoomed out of the etch front at the left part of Fig. 1 viewed along [110] direction parallel to the wafer surface. The smooth area (denoted as "B") exhibits a large number of fine step lines in parallel which are composed of planes of the {111} and {211} group. Two of them, arbitrarily chosen, are marked as white lines. During the etching process these steps move in $[1\bar{2}1]$ direction. The point S_u on the etch bottom denotes the kink site generation point, from which the steplines originate. Hence, line 2 marks a stepline which was generated earlier than line 3.
The rough side surfaces, denoted as area A, are residues of the peeling process caused by the stability of the near {111} planes. The angle $\beta = 54.7°$ is the characteristic and well known inclination of the {111} planes.

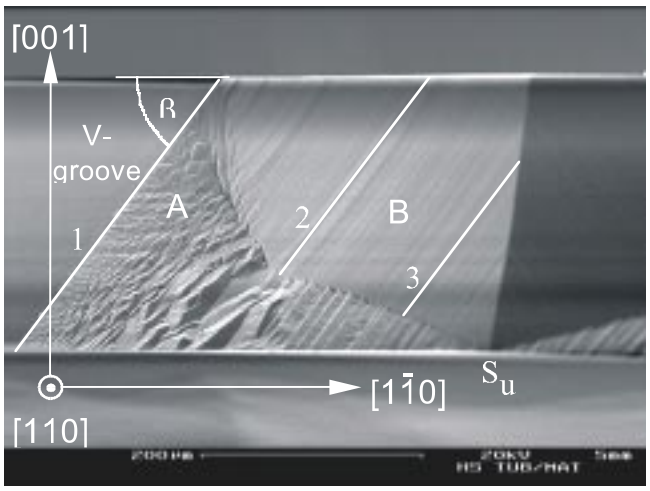

Fig. 2: SEM micrograph of a CC viewed along <110> direction showing fine steplines on area B directed parallel to the line 1 that separates area A from the {111} plane of the V-groove.

2.2 Simulation Method

The mathematical method used in our simulation approach had originally been developed for digital image processing and was then adapted to the purpose of efficient topography simulation [8,9]. The basic idea is to represent the etch body and its exterior as a black- white image (black = material, white = no material) which is altered by the action of certain set operations.

Each time step of an etching process is modelled as so-called "Minkowski subtraction" or "erosion operation", where a properly chosen "structuring element" acts on the etch body to mark all material that has to be removed next. The structuring element is a three-dimensional body, such as a sphere or an ellipsoid, the shape of this has to be adjusted to the specific etching mechanism under consideration. The geometrical configurations during the etch process are described by a cellular representation in order to ensure an efficient numerical implementation. To this end, the simulated region is discretized by a partition in equally shaped volume elements ("cells") labelled by a material index which indicates their location inside or outside of the etch body. The time evolution of the etch front is represented by the temporal change of the material indices of the cells which, in turn, is controlled by the structuring element as follows:

The structuring element is shifted parallel to the current etch front (i.e. the momentary surface cells, cf. Fig. 3). If the center of a cell is touched by the structuring element, this cell is marked for removal. In the following etch step, the set of all marked cells is abraded by turning their material index into the index of the etchant.

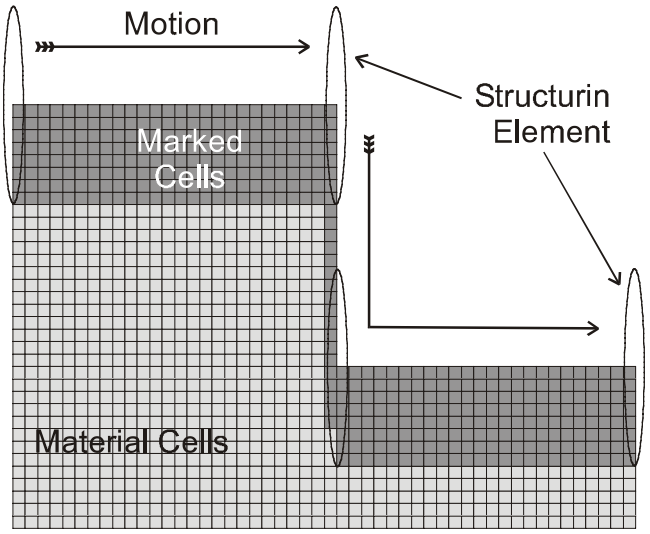

Fig. 3: Schematic sketch of the "erosion algorithm" using an ellipsoid as structuring element. The cells in dark gray are removed in the following etch step.

Fig. 3 illustrates the principle of the erosion operation by a two-dimensional schematic example. The center of the structuring element, an ellipsoid, is placed closely above each surface cell of the material region. All material cells are marked, if their centers are located in the interior of the structuring element. The marked cells are drawn in dark gray in Fig. 3, the structuring element is shown at four special positions on the etch front, and the arrows indicate the "motion" of the structuring element along the surface. Evidently, the elliptic shape causes an anisotropic etch rate, which is smaller in horizontal direction than in vertical direction.
We adapted this method for the implementation of our step flow model. However, in the case of orientation-dependent etching the simple classification in material and non-material is not sufficient, but additional crystallographic information of the location of a cell in the crystal structure must be assigned to each cell. A multi-valued index characterizes the particular etching behavior of each

individual cell. In this way, the simulation of substrates containing layers of different materials can be efficiently carried out. The method is very flexible and allows for realistic three-dimensional etch bodies. It also offers the possibility of simulating the etching of pre-structured wafers obtained, e.g., by laser micromachining or other etching processes (RIE, plasma etching), as well as double-sided wafer etching.

The structuring element in the case of orientation-dependent etching is determined by an etch rate vector $\vec{v}$, which has to be evaluated on each surface cell. The orientation and the magnitude of this quantity at a given cell position on the etch front is derived from the specific properties of the respective cell which, in turn, result from the equations of motion of kinks and steps building the crystal surface. Fig. 5 is a zoom-in view of the area around point P_2 in Fig. 4 and shows an exemplary array of steps with their respective etch rate vector $\vec{v}_{110}$ in [110] direction between the two points S_0 and P_2 shown in Fig. 4.

2.3 Description of the Algorithm

Fig. 4 illustrates the simulation of the etch front on the "left side" of a CC etched in KOH/H_2O solution. A coordinate system is introduced to determine the location of the characteristic points P_2, S_0, S_u and the link to the measurable distances a and b, which is:

$$a = |\vec{r}_2| \tag{1}$$

$$b = |\vec{r}_2| - \frac{1}{\sqrt{2}}|\vec{s}_0| \tag{2}$$

The discretization of the simulated region is chosen coarser than the dimensions of the fine steps of area B subject to the computational resources available. Furthermore, the material discretization is performed on a simple cubic grid oriented along [110] direction to ensure compatibility with an alternative simulation tool. Therefore, the real shape and orientation of the fine steps visible in the SEM micrographs is not resolved, but the enfolding envelope area is calculated accurately. The etch rate vector of the real steps is decomposed into components along the [110]- and the [100] direction to obtain the correct surface orientation of area B. It is notable that the interaction between two areas B coming from different CCs and contacting each other is accurately described.

Eq. (3) gives the correlation between the etch rate of the {121} group and a step etch rate $|\vec{v}_{110}|$ which is used in the simulation:

$$|\vec{v}_{110}| = \frac{|R_{121}|}{\sqrt{2}} ? \frac{2b}{\sqrt{(a-b)^2 + b^2}} \tag{3}$$

The simulation starts with detecting unstable points of the etch front. In the case of a masked planar wafer as initial condition, these crucial points are induced by the mask edges. The volume cell beneath a mask edge is classified as a kink site, which determines the special etching behavior of this cell.

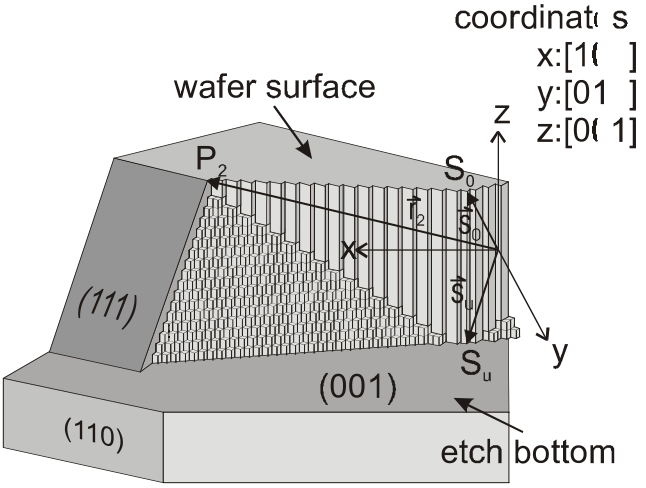

Fig. 4: Simulated etch front on the "left side" of the CC in Fig. 1. The etch mask is removed.

The cells containing kink sites are etched first and their adjacent cells in [110] direction are identified as belonging to a fine step of a B-type area. Consequently, these cells are etched with a step etch rate $\vec{v}_{110}$ in [110]-direction.

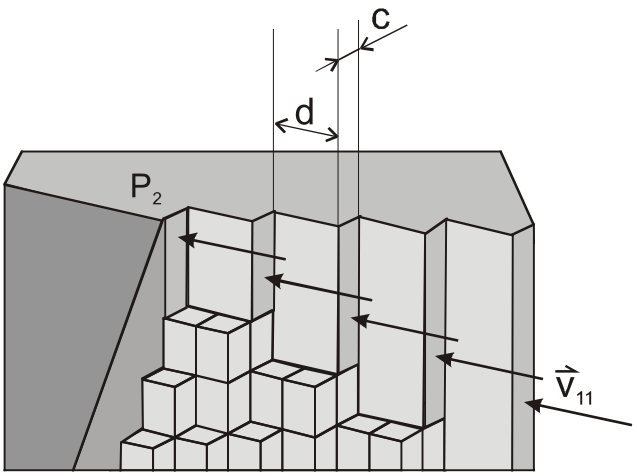

Fig. 5: Detailed view on the area at point P_2 showing the step dimensions c and d of the fine-stepped area B and the step etch rate $\vec{v}_{110}$ in [110]-direction.

Proceeding this way, the existing steps are etched and, simultaneously, new kink sites are created at the intersection of underlying {111} planes. Likewise, the etching of the [100] oriented bottom causes the appearance of new kink site cells at the point S_u, (see Fig. 4).
The relation of the step dimensions *c* and *d* in Fig. 5 is given by Eq. (4):

$$\frac{c}{d} = \frac{a}{b} - 1 \qquad (4)$$

The step dimensions and step etch rates $\vec{v}_{110}$ can be derived from the measured characteristic distances *a* and *b* introduced in Eq. (1) and Eq. (2).

3 RESULTS

Fig. 6 shows the simulation result of an underetched convex corner in {100}-Silicon exposed to a KOH/H_20 solution. The typical morphology observed along underetched convex corners is reproduced by our simulation as illustrated by comparison with the SEM micrographs in Fig. 1 and Fig. 2. The finely and regularly stepped "B" areas are reproduced in the simulation as well as the coarse "A" areas, which are formed by stepped residues. We can also clearly identify the {100} wafer surface, the {100} bottom and the stable {111} planes. Please note that, in a post-processing step, the discretization of the structure at {111} planes was smoothed for better visualization.

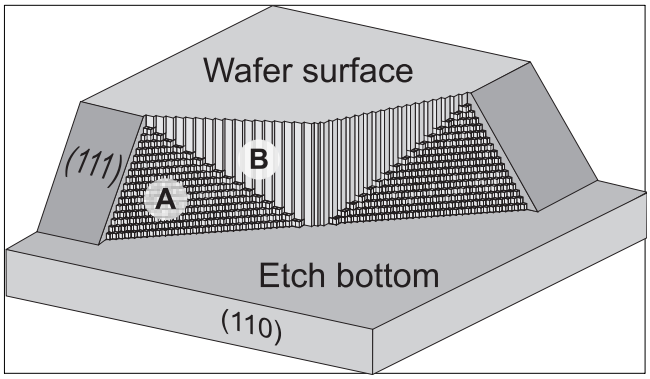

Fig. 6: Simulated etch front of a convex corner etched in pure KOH with 33 w% at 80°C (mask is removed).

4 CONCLUSION

We conclude that the shape and morphology of anisotropically etched structures observed in experiments agree with the predictions of the new "step flow model of 3D structuring". Thus it provides a solid basis for the predictive simulation of progressively complex MEMS structures, which allows for the efficient design of complicated etch mask compensation structures. Our three-dimensional simulation tool reproduces the details of the observed morphology like terraces and steps and can easily incorporate other materials and structuring techniques.
Moreover, employing methods adapted from digital image processing, we can keep the simulation times short and the computational effort affordable, even for three-dimensional process simulation.

Acknowledgement

The authors are very grateful to Professor Dr. S. Selberherr and Dipl. Ing. W. Pyka from the Institute for Microelectronics, Technical University of Vienna, for providing valuable assistance and support in the field of topography simulation.

REFERENCES

[1] Séquin, C.H., Sensors and Actuators, A, 34, pp. 225-241, 1992.

[2] Shepherd, J. N., MME '90 , Micromechanics Europe 1990, 2nd Workshop on Micromachining, Micromechanics and Microsystems, Berlin, 26-27.11.1990, Tech. Digest, pp. 241-246, 1990.

[3] Frühauf, J., Trautmann, K, Wittig, J, Zielke, D., J. Micromech. Microeng., 3, 3, pp. 113-115, 1993.

[4] Heim, U., Ph.D. Thesis, Technical University of Ilmenau, 1996.

[5] Allongue, P., Brune, H., Gerischer, H., Surf. Sci., 275, pp. 414, 1992.

[6] Allongue, P., Costa-Kieling, V., Gerischer, H., J. Electrochem. Soc., 140, pp. 1009-1018, 1993.

[7] Schröder, H., Obermeier, E., Workshop on Physical Chemistry of Wet Chemical Etching of Silicon, Holten, 17.-19.05.1998, Tech. Digest., pp 31-32, 1998

[8] Strasser, E., Selberherr, S., IEEE Trans. On Com.-Aided Design of Integrated Circuits and Systems, Vol.14, 9, pp 1104-1114, 1995.

[9] Strasser, E., Selberherr, S., SISDEP-93, Vienna, Austria, in Simulation of Semiconductor Devices and Processes, Eds.: S. Selberherr, H. Stippel, E. Strasser (Springer Verlag, Wien, 1993) pp. 357-360, 1993.